Inventory of supplemental information

Supplementary Experimental Procedures:

This section provides a detailed list of all reagents used for this study and also includes detailed descriptions of all experiments performed.

Supplementary Figures:

Figure S1: Supplements Figure 1, illustrates the results of TRIM9 and Mena colocalization experiments.

Figure S2: Supplements Figure 2, illustrates the results of EVL and Mena ubiquitination assays in HEK cells, VASP ubiquitination assay in HEK cells in the absence of DCC overexpression and ubiquitination assays of VASP single, double or triple lysine mutants.

Figure S3: Supplements Figure 3, illustrates that TRIM9 dependent regulation of filopodia density is downstream of DCC and that Mena and EVL localization to filopodia tips is not TRIM9 or netrin-1 dependent.

Figure S4: Supplements Figure 4, illustrates that TRIM9 dependent regulation of filopodial density is cytoskeletal and specifically downstream of the guidance molecule netrin-1.

Figure S5: Supplements Figure 5, illustrates that VASP or VASP K-R mutant overexpression in *TRIM9*$^{-/-}$ cortical neurons does not increase filopodia density.

Figure S6: Supplements Figure 6, illustrates filopodial protrusion dynamics are not dependent on TRIM9.

Figure S7: Supplements Figure 7, illustrates that *TRIM9* deletion does not alter the width of fimbria or the density of dendritic spines *in vivo*.

Supplementary Movies Legends:

Movie S1: Supplements Figure 1, demonstrates transient colocalization of TRIM9 and VASP at filopodia tips.

Movie S2: Supplements Figure 1, demonstrates prominent colocalization of TRIM9 lacking the RING domain and VASP at filopodia tips.

Movie S3: Supplements Figure 1, demonstrates colocalization of TRIM9 and Mena within filopodia.

Movie S4: Supplements Figure 6, demonstrates TRIM9 regulated and netrin-1 induced filopodial dynamics.

Movie S5: Supplements Figure 6, demonstrates FRAP experiment and VASP mobility at filopodia tips.

Movie S6: Supplements Figure 7, demonstrates *TRIM9*$^{+/+}$ cortical axon turning up a netrin-1 gradient.

Movie S7: Supplements Figure 7, demonstrates *TRIM9*$^{+/+}$ cortical axon turning down a gradient of the deubiquitinase inhibitor, PR-619.

Supplementary References:

This section provides a list of references cited in the supplementary experimental procedures section.

Supplementary Information:

Supplementary Experimental Procedures

Plasmids, antibodies and reagents: Plasmids encoding human TRIM9 cDNA, TRIM9ΔRING (aa139-781), and TRIM9ΔCC (removed aa220-394) were described previously (Winkle et al., 2014). TRIM9L316A was made using QuikChange site-directed mutagenesis of Leu316 to Ala. GFP-VASP individual, double or triple lysine mutants (K252R, K321R, K283,286R, K283,286,321R) were made using QuikChange site-directed mutagenesis. Simultaneous mutation of 9 lysine residues to arginine (K240,252,283,286,321,348,357,358,363R) in GFP-VASP (VASP K-R) was synthesized by gBlocks® Gene Fragment (IDT). The following plasmids were acquired: mCherry (Clonetech), FLAG-Ub (Dr. Ben Philpot, UNC-Chapel Hill), pCAX-eGFP-FPPPP-Mito, pCAX-eGFP-APPPP-Mito, pmscv-eGFP-Mena, pCaxeGFP-Mena+, pmscv-eGFP-EVL, pGEX-6P-1-CC, pGEX-6P-1-BBoxCCCos, pGEX-6P-1-BBoxCC, pGEX-6P-1-BBox, pGEX-6P-1-ΔSPRY, pGEX-6P-1-EVH1, pQE-EVH1, pGEX-6P-1-EVH2, pGEX-6P-1-Pro (Dr. Frank Gertler, MIT), peGFP-N1-VASP (Dr. Richard Cheney, UNC). TRIM9 FN3 domain sequence was cloned into the pGEX-6P-1plasmid. Antibodies include: TRIM9 rabbit polyclonal (generated using murine TRIM9 recombinant protein aa158-271), rabbit polyclonal antibodies against VASP and Mena (Dr. Frank Gertler, MIT), rabbit polyclonal against VASP (sc-13975, SCBT) mouse monoclonal c-Myc (9E10 SCBT), rabbit polyclonal GST (G1417 Sigma), mouse monoclonal against human βIII Tubulin (TujI SCBT), rabbit polyclonal against GFP (A11122 Invitrogen), mouse monoclonal against GFP (75-131 UC Davis Neuromab), chicken polyclonal against GFP (GFP-1010, aves LABS, inc.), goat polyclonal against GFAP (sc-6170 SCBT) mouse monoclonal against HA (05-904 Millipore), Penta His antibody (34660, Qiagen), ubiquitin (sc-8017, SCBT) and GAPDH (sc-166545, SCBT). Fluorescent secondary antibodies and fluorescent phalloidin labeled with AlexaFluor 488, AlexaFluor 568, or AlexaFluor647 were from Invitrogen. Recombinant netrin-1 was concentrated from HEK293 cells (Lebrand et al., 2004; Serafini et al., 1994). PR-619 ((2,6-diaminopyridine-3,5-bis(thiocyanate), abcam), MG132 (81-5-15, American Peptide Company), CytoD (Sigma-Aldrich, C8273), Rhodamine B isothiocyanate–Dextran (Sigma-Aldrich, R9379). siGENOME mouse VASP siRNA SMARTpool and siGENOME non-targeting siRNA pool #2 were purchased from Dharmacon.

Yeast two hybrid: LexA two-hybrid system selection with mouse Matchmaker cDNA library and beta-galactosidase assays were performed according to the manufacturer's protocol (Clontech). DCC was used as bait in an embryonic mouse brain library.

Selection of HEK 293 *TRIM9*$^{-/-}$ cells generated by CRISPR/Cas9 technology: The generation of HEK 293 *TRIM9*$^{-/-}$ cells was done by CRISPR/Cas9 gene editing using a guide RNA targeting the sequence 5-GCGGCTATGGCTCCTACGGGGGG-3' (hg19 chr14: +51561408 - 51561431) in exon 1 of the *TRIM9* gene in 293 cells. 5 x 10^5 HEK293 cells were transfected in 6-well plates with an expression plasmid (3 µg DNA/9 µl TranIT transfection reagent (Mirus Bio, Madison, WI) coding for a CMV promoter-driven CAS9-2A-RFP cassette and the U6-driven guide RNA. After 24 h RFP-positive cells were sorted by flow cytometry and limiting dilution cloning was performed by plating 0,5 RFP-positive cells in each well of 96-well plates. Growing clones were expanded. Genomic DNA was extracted using QuickExtract™ DNA extraction solution (Epicentre) and the target region of interest in was amplified by PCR (forward primer 5'-CACAGAGCTAGCGCCTCTC-3'; reverse primer 5'-TACGCGATTCTTGGGGAAGC-3'). After a pre-screening using the mismatch-sensitive T7 endonuclease I (T7EI) assay (Kim et al., 2009) positive clones in the T7 assay were sequenced. Knock-out cell clones were identified as cell clones harboring mono-allelic (clone 1) or all-allelic

(clone 2) frameshift mutations. Genotypes of the respective knockout cell lines are available upon request.

Transfection procedures: For transfection of plasmids and VASP or control Scramble siRNA (1 μM), neurons were resuspended after dissociation in Lonza Nucleofector solution (VPG-1001) and electroporated with an Amaxa Nucleofector according to manufacturer protocol. Since expression of FP4Mito blocks filopodia formation and neuritogenesis (Gupton and Gertler, 2010), pCAX-eGFP-AP4Mito or pCAX-eGFP-FP4Mito were transfected after neurons were cultured for 24 hours in vitro (once neurites had formed) using CalPhos™ Mammalian Transfection Kit (Clontech Laboratories, Inc.) according to manufacturer protocol with slight modifications. Briefly, 2μg of DNA was incubated with Solution A and B for 20 min. This mixture was added to neurons after the culture medium was replaced with neurobasal medium and allowed to incubate for 45 min. Following incubation, fresh neurobasal medium was added to the cells, allowed to incubate for another hour following which neurobasal media was replaced with fresh culture media. HEK cells were transfected using Lipofectamine 2000 (Invitrogen) as per manufacturer protocol.

Binding Assays: For binding assays, all recombinant GST-tagged proteins were purified by chromatography on sepharose-immobilized glutathione beads (ThermoScientific). For binding to endogenous TRIM9 or Ena/VASP, E15.5 mouse cortices were lysed in 1% NP40 lysis buffer (50 mM Tris pH7.5, 200 mM NaCl, 1% NP-40 with phosphatase and protease inhibitors). Lysates were pre-cleared with GST-glutathione-sepharose beads for 1 hour at 4°C with agitation and incubated with 5-10 μg of GST fusion protein or GST immobilized onto glutathione-sepharose beads at 4°C overnight. For EVH1 direct binding assay, His-EVH1 was expressed in *E. Coli* strain BL21 (DE3) Codon Plus (Agilent), bound to Ni-NTA beads and then eluted (Elution buffer: 50 mM Na_3PO_4 pH 8.0, 500 mM NaCl, 10 mM β-mercaptoethanol, 0.1% Tween-20, 10 mM Imidazole) and dialyzed. 50 nM concentrations of His-EVH1 and 50 nM of GST fusion TRIM9 and TRIM9 domains or GST immobilized onto glutathione-sepharose beads were incubated in PBS buffer (140 mM NaCl, 2.7 mM KCl, 10 mM Na2HPO4, 1.8mM KH2PO4, pH 7.4 plus protease inhibitors) as described in Li et al., 2001 at 4°C overnight. For FP4 competition assay 10 nM His-EVH1, 10 nM GST-CC and 0-100 nM FP4 were incubated in PBS buffer at 4°C overnight. For binding of Myc-tagged TRIM9 variants, HEK293 cells were transfected and 24 hours later lysed in 1% NP40 lysis buffer and incubated overnight at 4°C with 100 nM GST or GST-EVH1. For all binding assays, precipitated beads were washed three times with lysis buffer or PBS buffer and bound proteins were resolved by SDS-PAGE and analyzed by immunoblotting.

Preparation of lysates for ubiquitination and dimerization assays: For ubiquitination assay MG132 and netrin-1 or netrin-1 and PR-619 treated cells were lysed in IP buffer (20 mM Tris-Cl, 250 mM NaCl, 3 mM EDTA, 3 mM EGTA, 0.5% NP-40, 1% SDS, 2 mM DTT, 5 mM NEM (N-ethylmaleimide), 3 mM iodoacetamide, protease and phosphatase inhibitors pH=7.3-7.4). For 5-6 million cells 270 ul of ubiquitin IP buffer was added and incubated on ice for 10min. Cells were removed from the dish and transferred into tubes. 30 μl of 1X PBS was added and gently vortexed. Samples were boiled immediately for 20 minutes, until clear, then centrifuged at 14,000 rpm for 10 minutes. The boiled samples were diluted using IP Buffer without SDS to reduce the SDS concentration to 0.1%. For TRIM9 dimerization assay, HEK 293 cells transfected with Myc-tagged TRIM9 or TRIM9 variants and GFP tagged TRIM9 were lysed with RIPA buffer (50 mM Tris-HCl, ph 7.5, 150 mM NaCl, 1% NP40, 0.5% Sodium deoxycholate, 0.1% SDS with phosphatase and protease inhibitors).

Co-immunoprecipitation and Immunoblotting

For co-immunoprecipitation assays, IgG-conjugated A/G beads (SCBT) were utilized to pre-clear lysates for 1.5 hours at 4°C with agitation. Myc antibody-conjugated A/G beads (SCBT) or Protein A/G beads (SCBT) coupled with a mouse anti-GFP Ab (Neuromab) or rabbit anti-VASP Ab (SCBT) were agitated within pre-cleared lysates overnight at 4°C to precipitate target proteins. Beads were washed three times with lysis buffer and bound proteins were resolved by SDS-PAGE and analyzed by immunoblotting.

Neuronal culture preparation for imaging: Netrin-1 treated cells were fixed in 4% paraformaldehyde, permeabilized for 10 minutes in 0.1% TritonX-100, blocked for 30 minutes in 10% BSA, and stained with indicated primary antibodies for 1 hour at room temperature. Following three washes, species appropriate fluorescent secondary antibodies were added and allowed to incubate for 1 hour at room temperature. Following three washes, cells were mounted in a TRIS/glycerol/n-propyl-gallate based mounting media for imaging.

Microscope Descriptions: All live cell images and immunofluorescence images were collected on an Olympus IX81-ZDC2 inverted microscope equipped with the following objective lenses: a UPLFLN 40x/1.39NA DIC objective (Olympus), UAPON 100x/1.49NA DIC TIRF objective (Olympus), a 20x/0.85NA UPlanSApo DIC objective lens (Olympus), and a 4x/0.13NA Plan Apochromat objective (Nikon), an automated XYZ stage (Prior) and an Andor iXon EM-CCD. Images were procured using the Metamorph acquisition software. Neuroanatomical images were acquired on an inverted laser scanning confocal microscope (FluoView FV1200; Olympus) equipped with a 10X/0.4NA Plan Apochromat objective lens, a 20X/0.75NA Plan-Apochromat objective lens, and 488-nm and 561-nm argon lasers.

Colocalization and growth cone analysis: Pearson's correlation of colocalization between TRIM9 and Ena/VASP proteins was performed using regions of interest (ROI) drawn in filopodia and a Colocalization Test plugin for ImageJ with Fay randomization using images acquired with the 100x objective described above. Growth cone area, filopodia number, filopodia density and filopodia length were measured in ImageJ. Filopodia lengths were measured from the edge of lamellipodial veils to filopodia tips. For filopodia rescue assays, images of neurons expressing comparable levels of Myc(TRIM9 variants) were acquired with the 40x objective, and the number of growth cone filopodia recorded. TIRF imaging of TRIM9 and Ena/VASP proteins was performed after 48 hours *in vitro*, with the 100x objective and a solid state 491, 561 nm laser illumination at 100 nm penetration depth. Images were acquired every 0.5 seconds for 5 minutes. Similarly for GFP-VASP-K-R and mCherry VASP TIRF imaging, *TRIM9*$^{+/+}$ neurons were imaged after 48 hours *in vitro* either untreated or after 10 minutes of treatment with 9μM PR-619.

Filopodia dynamics measurements: For filopodial dynamics measurements, wide-field epifluorescence images of mCherry were acquired every 2.5 seconds for 5-10 minutes. 400 ng/mL netrin-1 was added 50 minutes prior to imaging netrin-1 treated neurons. Filopodial protrusion and retraction rates and phase durations were measured from kymographs as the slope and duration of individual events, respectively. In order to calculate the number of filopodia formed and lost, fluorescence images were first thresholded and then duplicated. Each frame was subtracted from the subsequent frame to generate a difference map, which was then used to count newly formed and lost filopodia. Filopodia lifetime was measured as the time from initial filopodial protrusion until retraction into the lamellipodial veil.

FRAP fluorescence recovery calculation: For FRAP assays neurons expressing GFP-VASP were imaged after 48 hours using 491 nm laser in TIRF mode every 0.5 seconds for 15 seconds, followed by a 1-second exposure with a solid state 405 nm laser in FRAP mode

(bleach spot ~1.25 μm in diameter), followed by imaging every 0.5 seconds with the 491 laser in TIRF mode for 60 seconds. Netrin-1 treated filopodia were imaged within 5 minutes of addition of 400 ng/mL netrin-1. DUB-inhibited filopodia were imaged within 30 minutes of addition of 9 μM PR-619. For analyzing FRAP imaging data, photobleaching was corrected by calculating an exponential decay from the last 30 seconds of imaging in a control region distant from the bleach spot ($F = F_0 * e^{-kt}$, where F is fluorescence, F_0 is initial fluorescence, k is the decay time constant, and t is time). Fluorescence recovery $t_{1/2}$ and % were calculated from an inverse exponential decay ($F = A*(1-e^{-\tau t})$, where F is fluorescence, A is recovery plateau fluorescence, τ is the recovery time constant, and t is time). The % recovery was calculated as the plateau fluorescence divided by the average pre-bleach fluorescence, and $t_{1/2}$ is the inverse of the recovery time constant τ. Both photobleaching and FRAP curves were fit to data using the Solver add-in of Microsoft Excel 2013.

Neuroanatomical imaging: All mice used for neuroanatomical studies were anesthetized with an intraperitoneal injection of 1.2% avertin and intracardially perfused with 4% paraformaldehyde (PFA). Brains were removed and fixed in 4% PFA for a subsequent 48 hrs , rinsed with 1x PBS and rested in 70% EtOH for 24 hours prior to vibratome or cryostat sectioning. For projection analysis in Nex-Cre/Tau$^{loxP\text{-}stop\text{-}loxP}$GFP mice, 100 μm coronal sections were cut and every other section was permeabilized in detergent solution (1x PBS + 0.1% Tx-100 + 0.2% Tween-20) for 1 hour on a shaker at RT. Sections were blocked in 10% BSA in 1x PBS for 5 hours, then placed in primary antibody solution (anti-GFP chicken (Aves ab1020) 1:2000, anti-GFAP rabbit (AbCam ab7260) 1:2500 in 1% BSA in PBS) for 24 hours on a shaker at 4°C. Primary antibodies were removed and sections were rinsed in 1x PBS for 1 hour prior to the addition of secondary antibody solution (AlexaFluor 488 chicken, Alexa fluor 561 or 647 rabbit + 1% BSA in 1x PBS) for 24 hours on a covered shaker at 4°C. After post-secondary rinsing with 1x PBS, sections were mounted in DPX mountant (VWR) and were imaged with the 10x objective on the LSCM described above. Brains from Thy1-GFP littermates were similarly prepared and imaged with the 20x objective on the LSCM described above. Cortical explants were imaged with the 4x objective described above.

Explant Analysis: Outgrowth was defined as total neurite pixels divided by the total number of pixels representing the neurite body. To measure biased outgrowth, explants were bisected in imageJ through the center of the explant orthogonal to the direction of the gradient. The number of pixels representing neurites on upgradient (U) and downgradient (D) were quantified in ImageJ. The guidance ratio was defined as (U−D)/(U+D), with a positive guidance ratio indicating attraction or biased outgrowth toward the netrin source. This analysis controls for growth-related effects (Mortimer et al., 2009; Rosoff et al., 2004).

Movie Legends:

Movie 1, related to Figure 1: TRIM9 and VASP colocalize at filopodia tips. TIRF time lapse imaging of GFP-VASP (red) and mCherry-TRIM9 in an axonal growth cone of a cortical neuron. Colocalization is observed in stable and dynamic filopodia tips. Time in seconds.

Movie 2, related to Figure 1: TRIM9ΔRING and VASP colocalize at filopodia tips. TIRF time lapse imaging of GFP-VASP (red) and mCherry-TRIM9ΔRING in an axonal growth cone of a cortical neuron. Colocalization is observed in stable and dynamic filopodia tips. Time in seconds.

Movie 3, related to Figure 1: TRIM9 and Mena colocalize within filopodia. TIRF time lapse imaging of GFP-Mena (red) and mCherry-TRIM9 in an axonal growth cone of cortical neuron. Colocalization is observed in stable and dynamic filopodia. Time in seconds.

Movie 4, related to Figure 6: Filopodial dynamics are affected by netrin-1 when TRIM9 is present. Time lapse imaging of soluble mCherry in axonal growth cones of *TRIM9*$^{+/+}$ (left) and *TRIM9*$^{-/-}$ (right) cortical neurons. 400 ng/mL netrin-1 was bath applied at 10 minutes (indicated in movie). Time in minutes:seconds.

Movie 5, related to Figure 6: FRAP assay of GFP-VASP at a filopodial tip. TIRF time lapse imaging of GFP-VASP in an axonal filopodium. Time is shown in seconds before (negative) and after (positive) bleaching by 405 nm laser.

Movie 6: Cortical axons turn up a netrin gradient, related to Figure 7. Time lapse DIC imaging of *TRIM9*$^{+/+}$ axons in the axon viewing chamber of the micropass gradient device turning up a gradient of netrin (left). Time lapse epifluorescence imaging of dextran gradient (middle) and a plot profile of the gradient (right) observed in the epifluorescence images. Time in minutes.

Movie 7: A gradient of ubiquitination is sufficient to induce axon turning, related to Figure 7. Time lapse DIC imaging of *TRIM9*$^{+/+}$ axons in the axon viewing chamber of the micropass gradient device turning down a gradient of PR-619 (left). Time lapse epifluorescence imaging of dextran gradient (middle) and a plot profile of the gradient (right) observed in the epifluorescence images. Time in minutes.

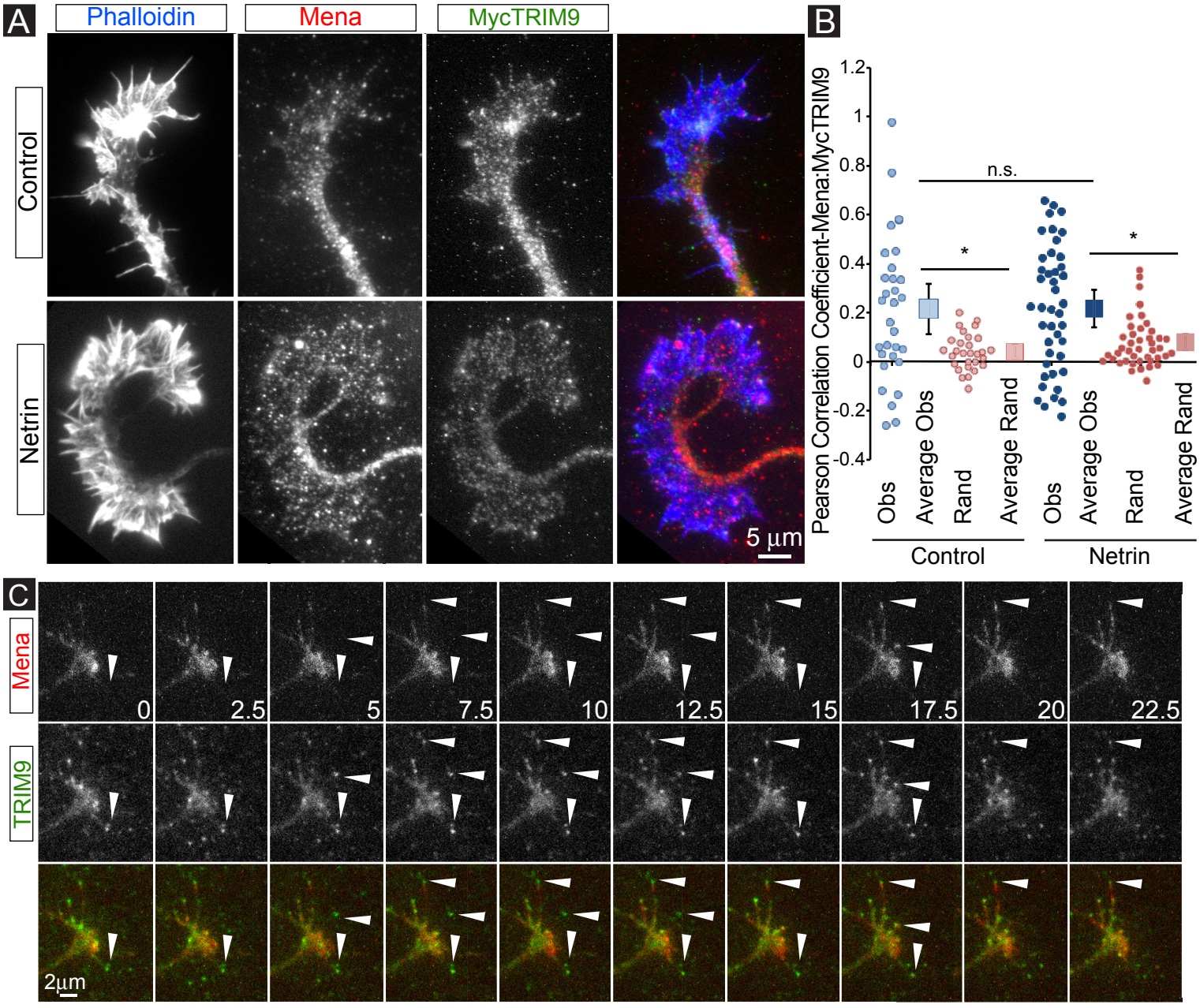
A
Phalloidin
Mena
MycTRIM9
Control
Netrin
5 µm
B
Pearson Correlation Coefficient-Mena:MycTRIM9
1.2
1
0.8
0.6
0.4
0.2
0
-0.2
-0.4
n.s.
*
*
Obs
Average Obs
Rand
Average Rand
Obs
Average Obs
Rand
Average Rand
Control
Netrin
C
Mena
TRIM9
0
2.5
5
7.5
10
12.5
15
17.5
20
22.5
2µm

Supplemental Figure Legends:

Figure S1, related to Figure 1: TRIM9 and Mena exhibit minimal colocalization: A) Axonal growth cones of control and netrin-treated cortical neurons stained for Mena (red), MycTRIM9 (green) and phalloidin (blue). **B)** Quantification of Pearson's Correlation Coefficient within filopodial regions (Obs = Observed measurements, Rand = pixels from one image randomized). Squares represent means +/- 95 % CI. **C)** Montage of TIRF images of GFP-Mena and mcherry-TRIM9, time in seconds. Arrowheads denote filopodia tips in which TRIM9 and Mena colocalize, time in seconds.

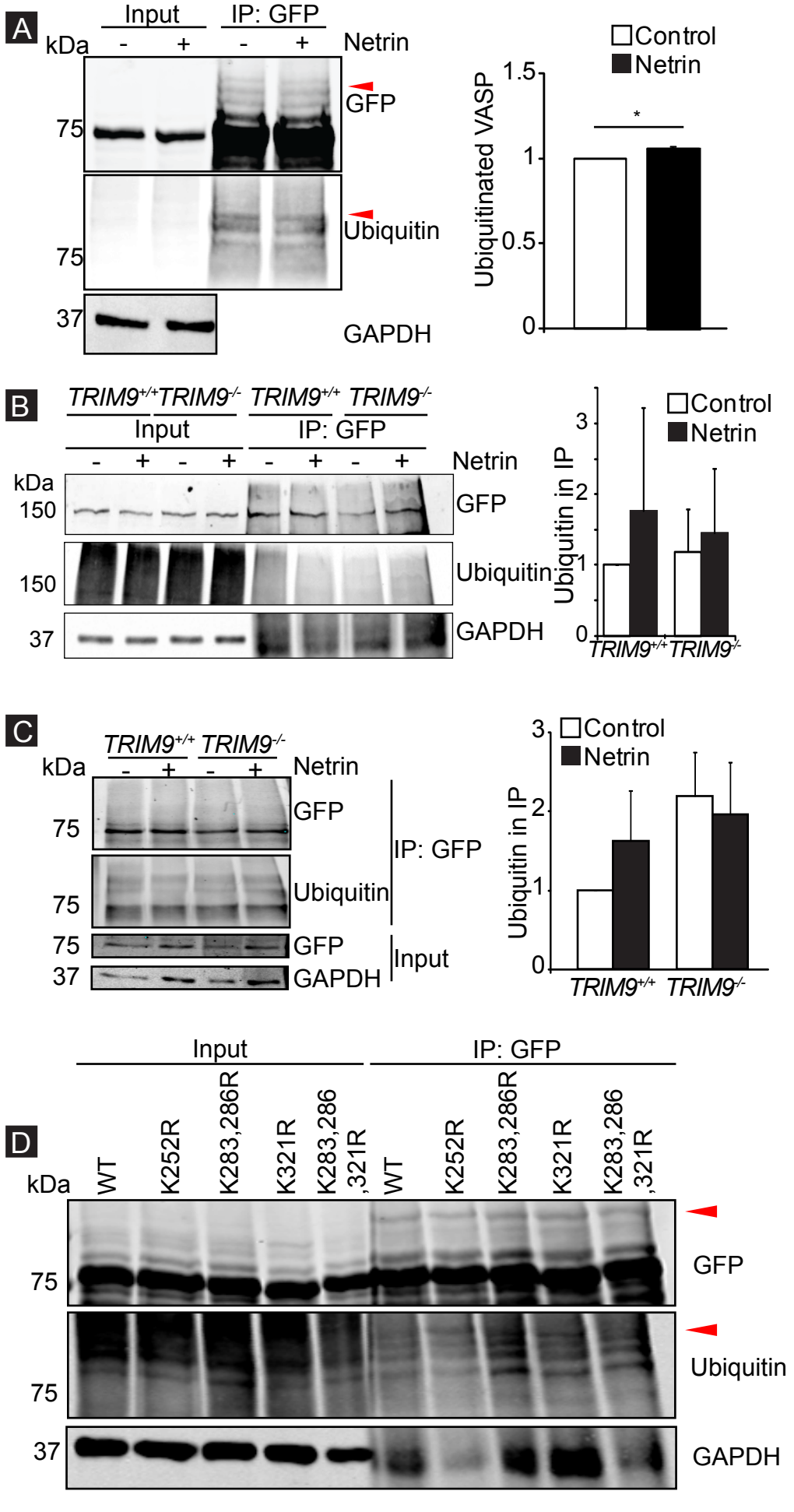
A
Input
IP: GFP
kDa
-
+
-
+
Netrin
75
GFP
75
Ubiquitin
37
GAPDH
Control
Netrin
Ubiquitinated VASP
1.5
1
0.5
0
*
B
TRIM9+/+
TRIM9-/-
TRIM9+/+
TRIM9-/-
Input
IP: GFP
Netrin
kDa
150
GFP
150
Ubiquitin
37
GAPDH
Control
Netrin
Ubiquitin in IP
3
2
1
0
TRIM9+/+
TRIM9-/-
C
TRIM9+/+
TRIM9-/-
kDa
Netrin
75
GFP
IP: GFP
75
Ubiquitin
75
GFP
Input
37
GAPDH
Control
Netrin
Ubiquitin in IP
3
2
1
0
TRIM9+/+
TRIM9-/-
D
Input
IP: GFP
kDa
WT
K252R
K283,286R
K321R
K283,286,321R
WT
K252R
K283,286R
K321R
K283,286,321R
75
GFP
75
Ubiquitin
37
GAPDH

Figure S2, related to Figure 2: Mena and EVL are not ubiquitinated by TRIM9 and VASP ubiquitination is not lost in the absence of DCC and is not reduced in single, double or triple VASP lysine mutants: A) GFP-VASP ubiquitination and quantification +/- SEM in the absence of DCC overexpression. No change in ubiquitination is detected upon netrin treatment. **B)** Mena ubiquitination assay and quantification +/- SEM in *TRIM9*$^{+/+}$ and *TRIM9*$^{-/-}$ HEK cells, GFP-Mena (~150 kDa). **C)** EVL ubiquitination assay and quantification +/- SEM in *TRIM9*$^{+/+}$ and *TRIM9*$^{-/-}$ HEK cells (~75 kDa). **D)** VASP ubiquitination assay with wildtype VASP and VASP K252R, K283,286R, K321R, K283,286,321R mutants. These mutants do not exhibit a reduction in the ~25kDa heavier VASP band that co-migrates with ubiquitin (red arrowheads)

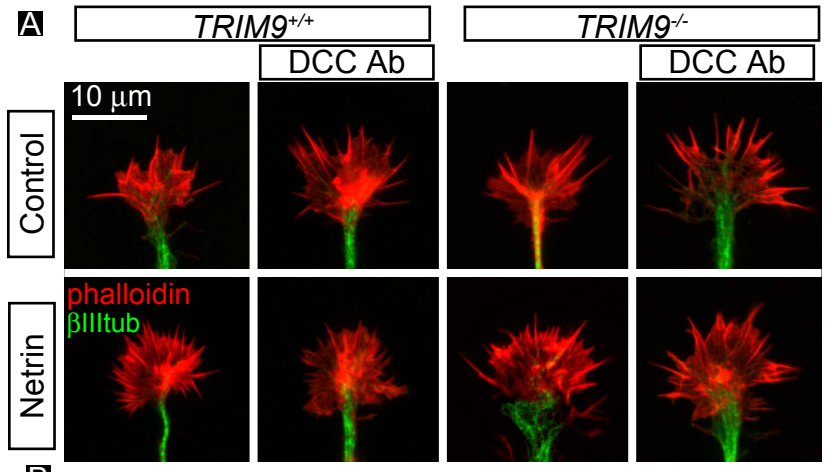
A
TRIM9+/+
TRIM9-/-
DCC Ab
DCC Ab
10 µm
Control
Netrin
phalloidin
βIIItub

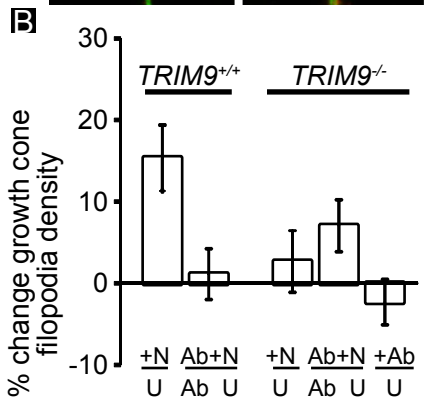
B
TRIM9+/+
TRIM9-/-
% change growth cone filopodia density
30
20
10
0
-10
+N
Ab+N
+N
Ab+N
+Ab
U
Ab
U
U
Ab
U
U

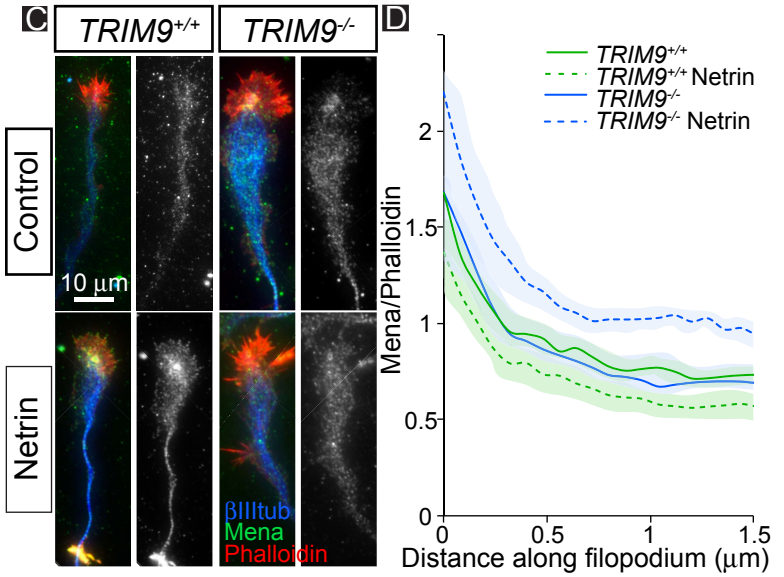
C
TRIM9+/+
TRIM9-/-
Control
Netrin
10 µm
βIIItub
Mena
Phalloidin
D
TRIM9+/+
TRIM9+/+ Netrin
TRIM9-/-
TRIM9-/- Netrin
Mena/Phalloidin
2
1.5
1
0.5
0
0
0.5
1
1.5
Distance along filopodium (µm)

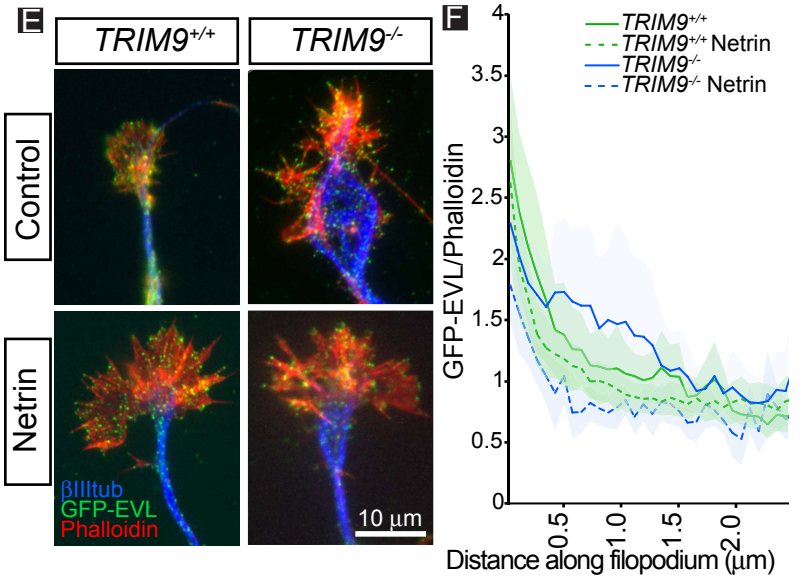
E
TRIM9+/+
TRIM9-/-
Control
Netrin
βIIItub
GFP-EVL
Phalloidin
10 µm
F
TRIM9+/+
TRIM9+/+ Netrin
TRIM9-/-
TRIM9-/- Netrin
GFP-EVL/Phalloidin
4
3.5
3
2.5
2
1.5
1
0.5
0
0.5
1.0
1.5
2.0
Distance along filopodium (µm)

Figure S3, related to Figure 3: TRIM9 regulation of growth cone filopodia occurs downstream of DCC: A-B) Images and quantification of filopodial density +/- SEM in *TRIM9*$^{+/+}$ and *TRIM9*$^{-/-}$ cortical growth cones treated with netrin, a DCC function blocking antibody (DCC Ab) or both. (+N/U: netrin-treated vs. untreated; Ab+N/Ab U: same comparison after pretreatment with DCC function blocking antibody; Ab/U: untreated vs. untreated after pretreatment with DCC antibody). **C)** Axonal growth cones from control and netrin-treated *TRIM9*$^{+/+}$ and *TRIM9*$^{-/-}$ cortical neurons, stained for Mena (green), βIII tubulin (blue) and phalloidin (red). **D)** Mena fluorescence intensity normalized to phalloidin +/- 95% CI from the tips of filopodia into the growth cone. **E)** Axonal growth cones from control and netrin-treated *TRIM9*$^{+/+}$ and *TRIM9*$^{-/-}$ cortical neurons, stained for GFP-EVL (green), βIII tubulin (blue) and phalloidin (red). **F)** GFP-EVL fluorescence intensity normalized to phalloidin +/- 95% CI from the tips of filopodia into the growth cone.

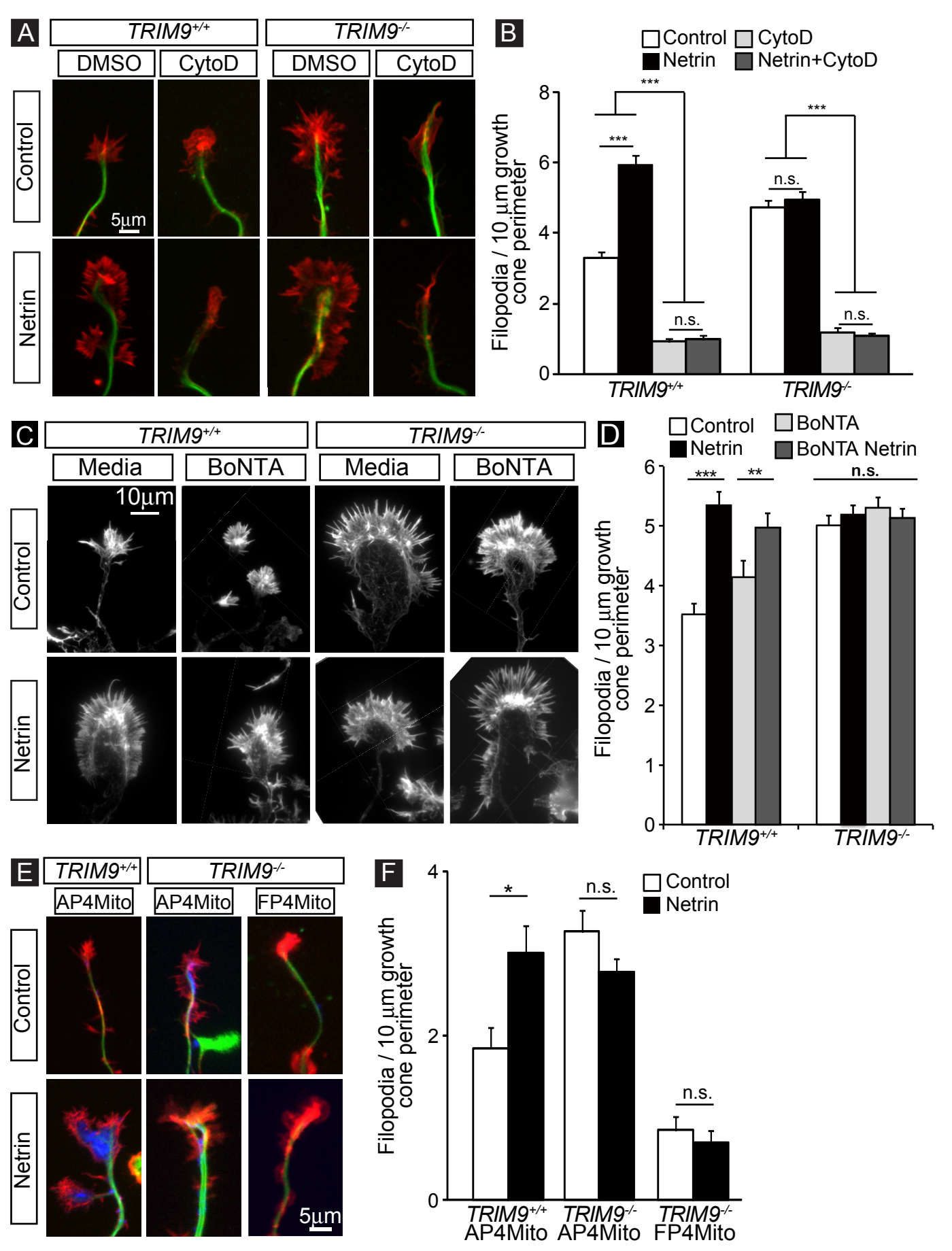
A
TRIM9+/+
TRIM9-/-
DMSO
CytoD
DMSO
CytoD
Control
Netrin
5µm
B
Control
CytoD
Netrin
Netrin+CytoD
Filopodia / 10 µm growth cone perimeter
***
***
n.s.
***
n.s.
n.s.
0
2
4
6
8
TRIM9+/+
TRIM9-/-
C
TRIM9+/+
TRIM9-/-
Media
BoNTA
Media
BoNTA
10µm
Control
Netrin
D
Control
BoNTA
Netrin
BoNTA Netrin
Filopodia / 10 µm growth cone perimeter
***
**
n.s.
0
1
2
3
4
5
6
TRIM9+/+
TRIM9-/-
E
TRIM9+/+
TRIM9-/-
AP4Mito
AP4Mito
FP4Mito
Control
Netrin
5µm
F
Control
Netrin
Filopodia / 10 µm growth cone perimeter
*
n.s.
n.s.
0
2
4
TRIM9+/+ AP4Mito
TRIM9-/- AP4Mito
TRIM9-/- FP4Mito

Figure S4, related to Figure 4: TRIM9-dependent filopodia density regulation is cytoskeletal and specific to netrin-1: A-B) Images and quantification of filopodia density +/- SEM in axonal growth cones from control (DMSO), CytoD, netrin or CytoD/netrin treated *TRIM9*$^{+/+}$ and *TRIM9*$^{-/-}$ neurons, stained for βIII tubulin (green) and phalloidin (red), n=2. **C-D)** Images and quantification of axonal growth cone filopodia density +/- SEM in control and netrin-treated *TRIM9*$^{+/+}$ and *TRIM9*$^{-/-}$ cortical neurons pre-treated with either media or botulinum toxin A (BoNTA), stained for phalloidin. **E-F)** Images and quantification +/- SEM of axonal growth cone filopodia density from control and netrin-treated *TRIM9*$^{+/+}$ and *TRIM9*$^{-/-}$ cortical neurons transfected with GFP-AP4Mito or GFP-FP4Mito, stained for GFP (blue), βIII tubulin (green) and phalloidin (red).

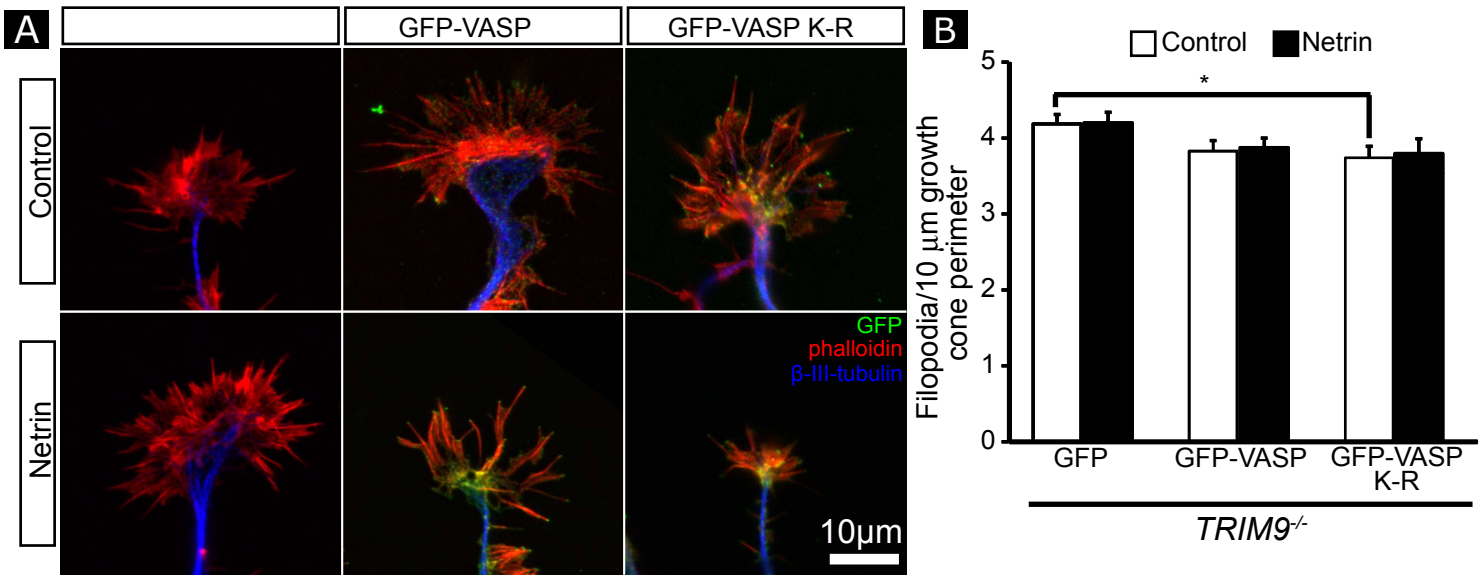
A
GFP-VASP
GFP-VASP K-R
Control
Netrin
GFP
phalloidin
β-III-tubulin
10μm
B
Control
Netrin
*
Filopodia/10 μm growth cone perimeter
0
1
2
3
4
5
GFP
GFP-VASP
GFP-VASP K-R
TRIM9-/-

Figure S5, related to Figure 5: Filopodia density is not increased by VASP overexpression in the absence of *TRIM9*: A) Axonal growth cones from control and netrin-treated *TRIM9*$^{-/-}$ cortical neurons expressing GFP, GFP-VASP or GFP-VASP K-R. **B)** Growth cone filopodia density +/- SEM from control and netrin-treated *TRIM9*$^{-/-}$ cortical neurons expressing GFP, GFP-VASP, or GFP-VASP K-R.

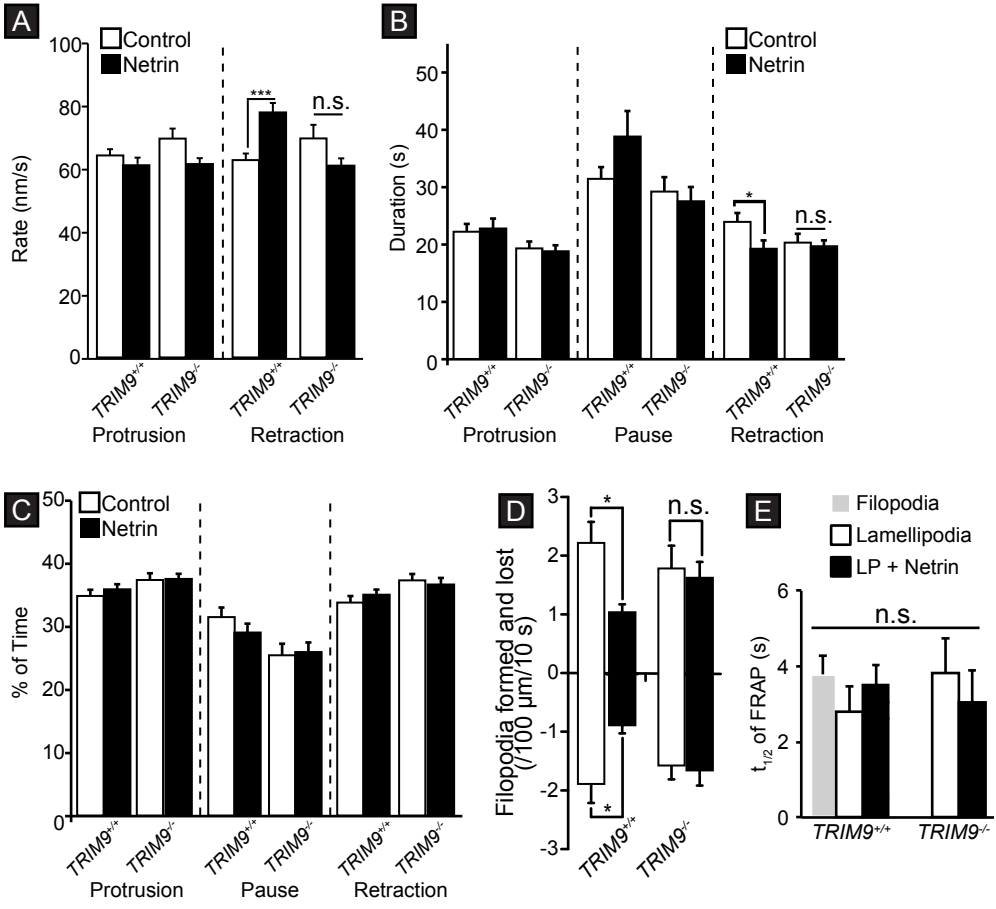
A
Control
Netrin
Rate (nm/s)
100
80
60
40
20
0
***
n.s.
TRIM9+/+
TRIM9-/-
TRIM9+/+
TRIM9-/-
Protrusion
Retraction
B
Control
Netrin
Duration (s)
50
40
30
20
10
0
*
n.s.
TRIM9+/+
TRIM9-/-
TRIM9+/+
TRIM9-/-
Protrusion
Pause
Retraction
C
Control
Netrin
% of Time
50
40
30
20
10
0
TRIM9+/+
TRIM9-/-
TRIM9+/+
TRIM9-/-
TRIM9+/+
TRIM9-/-
Protrusion
Pause
Retraction
D
Filopodia formed and lost
(/100 µm/10 s)
3
2
1
0
-1
-2
-3
*
*
n.s.
TRIM9+/+
TRIM9-/-
E
Filopodia
Lamellipodia
LP + Netrin
t1/2 of FRAP (s)
6
4
2
0
n.s.
TRIM9+/+
TRIM9-/-

Figure S6, related to Figure 6: Filopodial protrusion dynamics are not regulated by TRIM9: A) The rate of filopodial tip protrusion and retraction +/- SEM, the **B)** duration of time +/- SEM and **C)** percentage of time +/- SEM spent protruding, retracting or pausing measured from kymographs of growth cone filopodia, as shown in Figure 6. **D)** Frequency of filopodial formation and loss +/- SEM in *TRIM9*$^{+/+}$ and *TRIM9*$^{-/-}$ neurons before and after treatment with netrin. **E)** FRAP $t_{1/2}$ +/- SEM of GFP-VASP in lamellipodial regions.

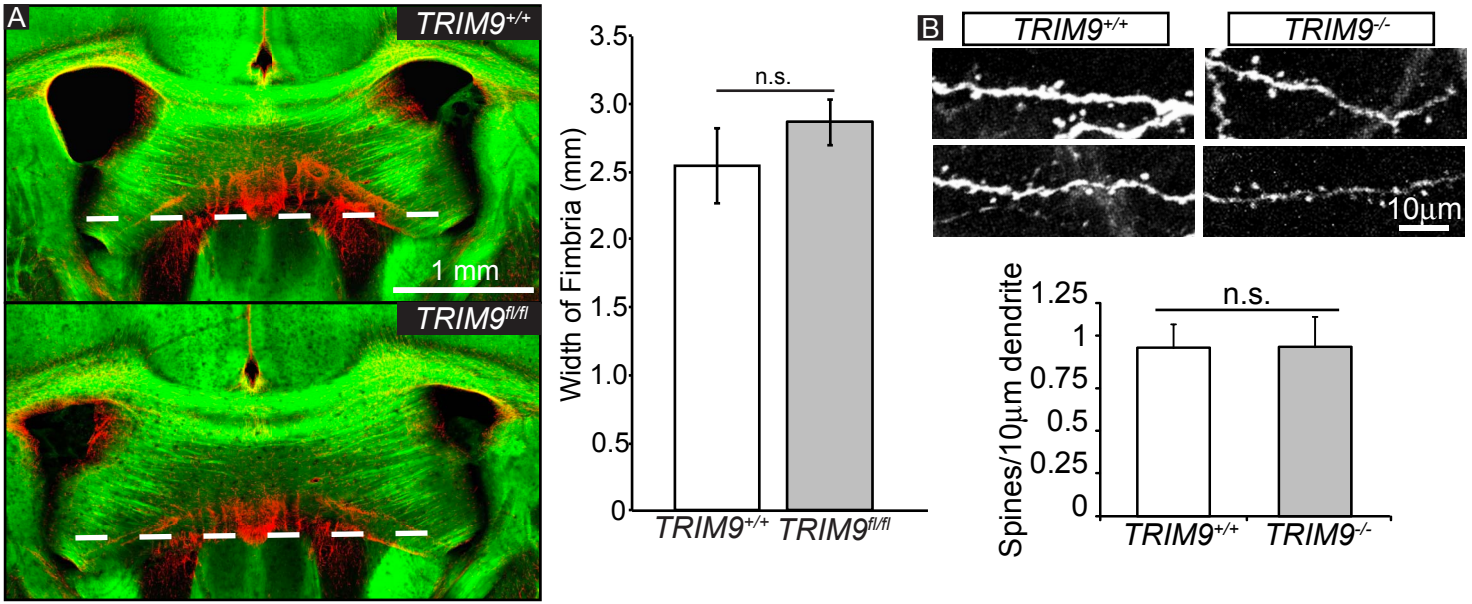
A
TRIM9+/+
1 mm
TRIM9fl/fl
Width of Fimbria (mm)
3.5
3.0
2.5
2.0
1.5
1.0
0.5
0
n.s.
TRIM9+/+
TRIM9fl/fl
B
TRIM9+/+
TRIM9-/-
10µm
Spines/10µm dendrite
1.25
1
0.75
0.5
0.25
0
n.s.
TRIM9+/+
TRIM9-/-

Figure S7, related to Figure 7: The fimbria and density of dendritic spines are not altered by deletion of *TRIM9*: A) Coronal sections from 5 week old Nex-Cre/Tau$^{loxP\text{-}stop\text{-}loxP}$GFP/ *TRIM9*$^{fl/fl}$ *and TRIM9*$^{+/+}$ littermates, demonstrating that the width of the fimbria does not significantly change between littermates, n=3 pairs of littermates, p=0.7. **B)** Example images of spines along a dendrite of GFP+ pyramidal cortical neurons from coronal sections of Thy1-GFP *TRIM9*$^{+/+}$ and *TRIM9*$^{-/-}$ P21 mice brains. Mean spine density +/- SEM is reported.

SUPPLEMENTARY REFERENCES

Gupton, S.L., and Gertler, F.B. (2010). Integrin signaling switches the cytoskeletal and exocytic machinery that drives neuritogenesis. Dev Cell *18*, 725–736.

Kim, H.J., Lee, H.J., Kim, H., Cho, S.W., and Kim, J.-S. (2009). Targeted genome editing in human cells with zinc finger nucleases constructed via modular assembly. Genome Res. *19*, 1279–1288.

Lebrand, C., Dent, E.W., Strasser, G.A., Lanier, L.M., Krause, M., Svitkina, T.M., Borisy, G.G., and Gertler, F.B. (2004). Critical role of Ena/VASP proteins for filopodia formation in neurons and in function downstream of netrin-1. Neuron *42*, 37–49.

Li, Y., Chin, L.S., Weigel, C., and Li, L. (2001). Spring, a novel RING finger protein that regulates synaptic vesicle exocytosis. J Biol Chem *276*, 40824–40833.

Serafini, T., Kennedy, T.E., Galko, M.J., Mirzayan, C., Jessell, T.M., and Tessier-Lavigne, M. (1994). The netrins define a family of axon outgrowth-promoting proteins homologous to C. elegans UNC-6. Cell *78*, 409–424.

Winkle, C.C., McClain, L.M., Valtschanoff, J.G., Park, C.S., Maglione, C., and Gupton, S.L. (2014). A novel Netrin-1-sensitive mechanism promotes local SNARE-mediated exocytosis during axon branching. J Cell Biol *205*, 217–232.